Pneumatic Actuator for Human Handling by Additive Manufacturing

Miguel Oliveira Meirinho Lopes Nabais
miguel.nabais@tecnico.ulisboa.pt
Instituto Superior Técnico, Universidade de Lisboa, Portugal
November 2017

ABSTRACT

Some people have pathologies, which are either congenital or acquired deformations. Those pathologies can be attenuated using new technologies. In this context, it is intended to develop a soft pneumatic actuator, for human handling/manipulation, with the use of advanced additive manufacturing. The work is developed using finite element analysis (FEA) and computer aided design (CAD) software. So, using the software combined with advanced additive manufacturing, one can physically get the actuator.
The material used in the 3D printing of the actuators, called NinjaFlex®, is tested with different printing parameters and is subjected to post-processing to achieve airtight pneumatic actuators. This post-processing ensures longer life to the actuator and improve the surface finish. Finally, a physical (functional) prototype of the pneumatic actuator and actuation system, is developed. With the computational results, a sensitivity analysis is performed, which allows to estimate the sensitivity of the results when changing a given parameter. It is shown that the parameters that most influence the bending / deformation of the actuator are: pressure, wall thickness, radius dimension and number of fundamental deformation elements. With the physical prototype and with the actuators it is also possible to calculate the gripping force. The grip control is based on the failsafe concept, in which, in the absence of actuation, the system remains in its position, for safety proposes.

KEYWORDS: Soft pneumatic actuator, airtightness, NinjaFlex®, 3D printing, additive manufacturing, functional prototype

1. INTRODUCTION

1.1. MOTIVATION

The manipulation of objects is essential for any human. There is a need for people to maintain their manipulation ability if in some case they have lost it. Engineers have the capacity to design solutions for people with this problem

3D printed Prosthetics have proven to be a successful option for people who need them. Not only on the cost level, but also on the level of comfort and utility.

In this work, a pneumatic actuator printed in 3D using flexible material, is presented. When subjected to internal pressure these actuators will bend resembling to a human finger. This paper presents an exploratory research that needs to be further developed so the actuator is shaped like a human finger. Through this, it is possible to show the potential of this technology.

1.2. OBJECTIVES AND MAIN CONTRIBUTIONS

The goal of this work is to develop a flexible pneumatic actuator for human manipulation, with the use of additive manufacturing. The work is also developed using finite element analysis software (FEA), computer aided design (CAD) and software that allows to convert STL files into G-CODE files. Thus, using these software programs and using an advanced additive manufacturing feature, the actuator is physically obtained.

Building on the work presented by Yap, Ng and Yeow, (2016), an identification of parameters that influence the response of the actuator, when subjected to internal pressure is performed and a new actuator is devised. For the geometric modelling of the actuator, the CAD software - SOLIDWORKS® is used. The

recognition of these parameters is done through the characterization of the actuator after a computational analysis using the finite element software - ABAQUS®. It is also possible to analyse the bending angle of the actuator, which is higher or lower, depending on the parameter that is changed. It is further predicted to develop a pneumatic actuator with a more anatomical geometry.

In this work the material used in the 3D printing of the actuators, called NinjaFlex®, is analysed and tested with different printing parameters, to obtain airtight pneumatic actuators.

Finally, the method to develop and build an experimental platform test - a physical prototype of the actuation system of the pneumatic actuator is also presented.

1.3. STATE OF THE ART

Animals have soft structures that allow them to move in complex natural environments. These capabilities have inspired engineers to incorporate flexible technologies into their designs. The goal is to provide robots with new bio-inspired capabilities that enable adaptive and flexible interactions with unpredictable environments (Kim, Laschi and Trimmer, 2013).

Soft robotics, or flexible robotics, is the area where flexible materials are used and in which mechanisms are implemented in order to allow the shape and stiffness of a device to be varied. This approach is considered radically transformative because it sets aside the basic assumptions of robotics. Overcoming these assumptions means that well-known theories and techniques of robotics are poorly applicable and that new solutions are needed. It is easy to understand that one of the problems in developing efficient robots is the lack of reliable and robust flexible actuators. However, promising new technologies are emerging with new flexible materials that represent the development of flexible actuators (Laschi and Cianchetti, 2014).

In 1976, Wilson obtained the patent for the *Simrit Finger*, (Wilson, 1988), a bellow-type actuator capable of controlling the bending movement. The walls of the actuator had undulations extending partially around the perimeter of the section, allowing asymmetric deformation when the inner chamber was under pressure.

Flexible robotic applications have great potential regarding medical devices because they ensure a synergistic and safe interaction with humans.

Some researchers at Harvard University have developed pneumatic actuators (ventricular assist devices - VADs) that allow a patient to get assistance when his heart is failing. It is placed around the heart, which is externally stimulated by the actuator in order to restore its function, (Payne *et al.*, 2017).

A portable shoulder was developed combining two types of actuators, which allow anatomical movements, adduction (AD) and abduction (AB) of the arm through the shoulder, and allow flexion (HF) and horizontal extension (HE), (O'Neill *et al.*, 2017).

Prostheses are accessible to few people due to their expensive cost. With the development of 3D printers, many prosthetic solutions were developed so that people could have a more comfortable life, at an affordable price.

With the technological advances, new materials have emerged, of which NinjaFlex® stands out. NinjaFlex® is a thermoplastic polyurethane (TPU), which produces flexible prints with elastic properties and is the material most used and studied in this thesis. It is a recent material (2013) of which there is still not much knowledge in 3D printing.

Researchers at the National University of Singapore have developed pneumatic actuators printed in 3D, using FDM technology with NinjaFlex® material. They are actuated with internal pressure, instead of using cables. When subjected to this internal pressure, they have the ability to bend. They also developed, with those actuators, a portable hand and wrist mechanism capable of assisting flexion of the fingers and wrist, (Yap, Ng and Yeow, 2016).

2. METHODS AND MODELS

Objects manipulation is essential for the daily life of any human being. In order to handle objects, man has to carrier healthy upper limbs.

The lack or loss of a limb may cause multiple problems, such as physical incapacity, need of prosthesis, pain, changes in body image among many others (Desmond and MacLachlan, 2006).

2.1. Computational Modelling of a Pneumatic Actuator

Using the study of Yap, Ng and Yeow, (2016) the pneumatic actuator that served as proof of concept for this thesis, Figure 2.1 was modelled in Solidworks®.

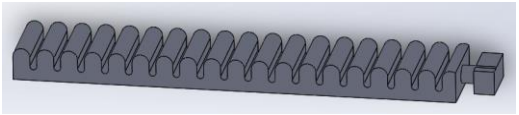

Figure 2.1 – Initial model of Yap, Ng and Yeow, (2016)

To improve the actuator, performance an increase its the flexion / bending angle, is needed when compared with the flexion / bending angle of the initial model. To do that, the Fundamental Element of Deformation (EFD), Figure 2.2, is developed and analysed.

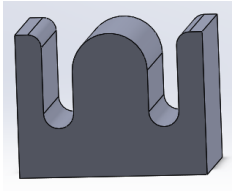

Figure 2.2 - Fundamental Element of Deformation (EFD)

To model an EFD, Solidworks software is used, and there are some variables to consider, Upper radius (R1), Lower radius (R2), Middle height (R1+f+R2), Width (w) and Height (h). The EFD length is determined by the radius (R1 and R2), Figure 2.3.

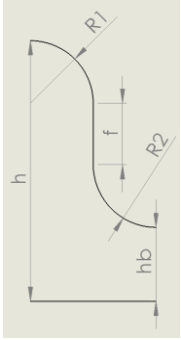

Figure 2.3 – EFD Modelling

Using the finite element software ABAQUS®, the deformation of the EFD and the complete actuator were analysed. With an iterative process, the actuator configuration was improved so that it deforms more with the same operating internal pressure. The improved geometry is presented in Table 2.1.

2.2. FEM Analysis and Results

From the iterative process mentioned above, it was obtained the configuration presented in the Table 2.1**.**

In Figure 2.4, the best EFD configuration is presented, and that is the configuration presented in Table 2.1.

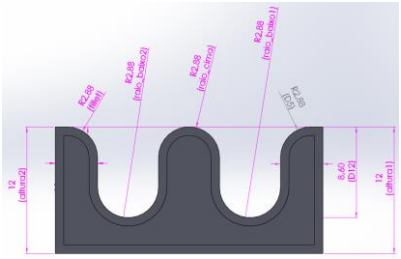

Figure 2.4 - EFD that causes larger bending angle

For a 2.5 bar pressure the EFD can deform 85.2°. Figure 2.5 shows the ABAQUS® software response to EFD shown in Figure 2.4.

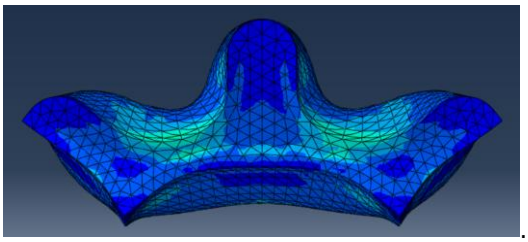

Figure 2.5 - ABAQUS® response to EFD presented in Figure 2.4

Thus, knowing the angle at which it is intended to bend the component it is possible to determine the number of EFD's required. Knowing the best configuration of the fundamental deformation element, it is now possible to analyse the behaviour of the complete actuator, with different numbers of EFD's, that is, with different lengths.

Table 2.1 - Iterative process with variables and system response – final configuration

Iteration (it)	Upper Radius (R1) [mm]	Lower Radius (R2) [mm]	Middle height (R1+f+R2) [mm]	Width (w) [mm]	Height (h) [mm]	Bending Angle (°) [degrees]
5.1	2.88	2.88	8.6	15	12	85.2

Table 2.2 – Computational response of the complete actuator, with different number of EFD's

Number of EFD's	Operating pressure [bar]	Actuator Length [mm]	Wall thickness [mm]	Bending Angle (°) [degrees]
3	2.5	75	1.2	157.2
4	2.5	98.08	1.2	201.9
5	2.5	121.15	1.2	247.4

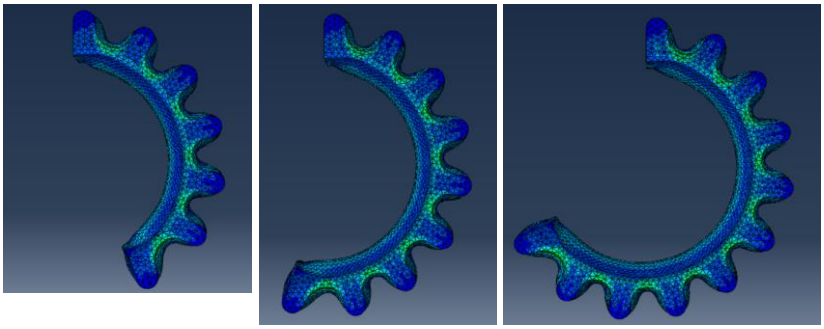

Figure 2.6 - Finite element analysis of the complete actuator, 3 EFD's (left), 4 EFD's (center), 5EFD's (right)

From Table 2.2, for the same operating pressure, the larger the number of EFD's the larger will be the bending angle of the actuator. The bending angle increases by 28.4% if the actuator has 4 EFD's instead of 3 and increases by 57.4% if the actuator has 5 EFD's instead of 3. Figure 2.6 shows how the bending angle of the actuator varies after internal pressure has been introduced, with the different numbers of EFDs presented.

Then, through the finite element method, the bending of the complete actuator for each of the configurations is compared, R1=R2=2.88mm, R1=R2=2mm and wall thickness equal to 0.8mm for both cases. The dimensions and results are presented in Table 2.3.

For analysis 1, the only change to be made in the model, compared to that presented in Table 2.2, is the decrease of the wall thickness from 1.2mm to 0.8mm. This reduction is made to compare identical actuators, because the actuator of analysis 2 has 0.8mm of wall thickness.

Analysis 2 shows a length almost equal to that of analysis 1, it is not possible to have an exactly equal length, because the radius are different and this is the closest value that is obtained. Neglecting the small difference in lengths, the only difference between analysis 2 and analysis 1 are the radius and the number of EDF's, as shown in Table 2.3. In analysis 2, there are 7 EFD's while in analysis 1 there are only 5, so for the same length, its introduced two more EDF's. The increase in the number of EDF's is a consequence of the smaller radius. This reduction of the radius translates into an increase of the bending angle, as shown in Table 2.3. The bending angle of the full actuator increases by 11.8% due to the values of the radius passing from 2.88mm to 2mm.

Table 2.3 - Response of the complete actuator with identical length, different radius and different number of EFD's

Analysis	Upper Radius (R1) [mm]	Lower Radius (R2) [mm]	Number of EFD's	Middle height (R1+f+R2) [mm]	Width (w) [mm]	Height (h) [mm]	Bending Angle (°) [degrees]
1	2.88	2.88	5	8.6	15	12	316.0
2	2	2	7	8.6	15	12	353,3

2.3. SENSITIVITY ANALYSIS

A sensitivity analysis of the system response to specific parameter perturbations allows to perceive the parameters that, when altered significantly change the system response and indicate how much the system response varies if the value of a given parameter is changed. To ensure that the numerical evaluation of the sensitivity of the response is performed correctly, different levels of perturbations are used to calculate the sensitivities.

In this analysis its intended to understand which parameters influence the system response, that is, which parameters cause larger bending of the actuator. For this, each parameter is perturbed independently, and a new analysis is performed, in order to evaluate the sensitivity of the result to this perturbance. The perturbed parameters, in the EFD analysis, are: pressure, wall thickness (wt) and width. The perturbed parameters in the complete actuator analysis are: length, number of EFD's (#EFD's) and radius variation (Δr's).

Sensitivities are expressed as the first derivative of a system's response with respect to the perturbed parameter. In this work, the bending angle is the response of the system, whereas the perturbed parameters are those previously mentioned. The first derivative is calculated using finite differences:

$$\boldsymbol{S} = \frac{\boldsymbol{O_P - O_0}}{\boldsymbol{I_P - I_0}} \qquad [2.1]$$

Where S is the sensitivity of the response, O_P and O_0 are the perturbed and unperturbed responses respectively and I_P e I_0 are the perturbed and unperturbed parameters respectively.

EFD Analysis:

Using the equation [2.1], presented above, the sensitivity of the response is calculated and the parameters that most influence response are the pressure, the wall thickness and the width.

If the internal pressure is increased by 1 bar, the EFD will, on average, increase by a further 12.6°.

If the wall thickness is increased by 1mm the bending angle will reduce, on average, 20.2°. Thus, if the wall thickness is reduced by 1mm, the EFD bending angle will, on average, increase 20.2°.

If the width is increased by 1mm, the EFD will, on average, increase 7.3°.

Complete Actuator Analysis:

Also using the equation [2.1], the sensitivity of the response is calculated and the parameters that most influence response are the number of EFD's and the radius dimensions.

For each EFD that is introduced into the actuator, it will, on average, bend more 45.1°.

If the radius dimension is increased by 1mm the bending angle will reduce, on average, 42.4°. Thus, if the radius dimension is reduced by 1mm, the actuator bending angle will, on average, increase 42.4°.

2.4. RESULTS DISCUSSION

The complete actuator consists of a certain number of EFD's (the number of EFD's influences the overall length of the actuator) and an addition that is made at its the end, Figure 2.7.

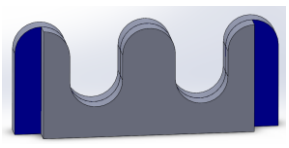

Figure 2.7 - EFD difference with and without addition

As seen previously, an EFD deforms 85.2°. Thus, for the complete actuator, if the response is linear, the bending angle is a multiple of 85.2°, such as $\Theta_{\#EFD's} = \#EFD's \times 85.2°$. Therefore, theoretically, $\Theta_3 = 255.6°$, $\Theta_4 = 340.8°$ and $\Theta_5 = 426.0°$. The results presented in Table 2.2 do not take into account the above-mentioned addition, which actually introduces a small decrease in the bending angle. The computational analysis of the EFD with addition allows to know the bending angle that it presents when subjected to internal pressure: $\Theta_{with\ addition} = 72.9°$. In the computational analysis of the complete actuator, to the value obtained in the response, it is necessary to add 85.2°-72.9° = 12.3° to be able to compare the computational response for a given number of EFD's with the theoretical response for the same number of EFD's.

Table 2.4 – Computational response of the complete actuator, with different number of EFD's taking into account the addition

Number of EFD's	Bending angle with addition (°) [degrees]
3	169.5
4	214.2
5	259.7

There is a clear difference between the theoretical and the computational values, explained below.

In the analysis of the EFD, if the response of the EFD is analysed, it is concluded that the tip of the EFD increases the rigidity of the system and this causes an increase of the curvature in this final zone of the EFD. There is a confluence of line 1 and line 2, that is, both converge towards the tip. Therefore, for line 1 converge to the same the EFD bends more, as can be seen in Figure 2.8.

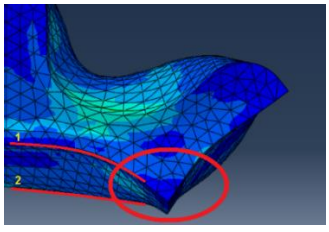

Figure 2.8 – EFD response analysis

In the analysis of the complete actuator, both lines follow the curvature, and at the end of the actuator happens the same phenomenon described above, Figure 2.9.

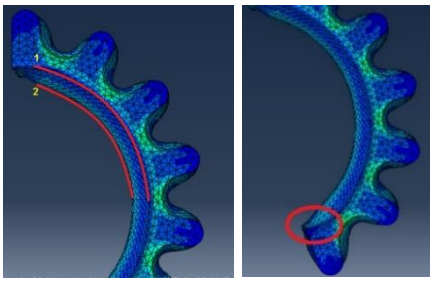

Figure 2.9 – Complete actuator response analysis

The referred phenomenon causes a difference due to an accumulation of errors proportional to the number of EFD's. The bigger the actuator, the later the lines 1 and 2 converge, so, if the value of an EFD, like this one, is used as theoretical value, that has associated "errors", the bigger will be the error in the analysis of this actuator.

3. Development of Pneumatic Actuators by Additive Manufacturing

In this chapter the ideal printing conditions, for NinjaFlex® material, as well as post-processing that are made to the actuators after they are printed, are presented so that the airtightness is guaranteed for a longer period of time. The models of the actuators developed along this work, the base model and the model with anatomical approximation are also presented.

3.1. NinjaFlex®

3.1.1. Ideal Printing Conditions

In this work the parameters concerning NinjaFlex® used in the Lulzbot® TAZ 6 printer are established in order to guarantee insolation of the chamber. A full description of these parameters can be found on the dissertation that supports this work.

3.1.2. Post-processing

Post-processing, in 3D printed materials, is very common. For rigid materials - Acetone vapor is a usual technique to improve the finishing of ABS printed parts. When the solvent is sparingly applied, it will dissolve only the outer surface resulting in a smooth, glossy finish, (Michael Graham, 2015). Dichloromethane, Ethyl Acetate or Tetrahydrofuran are used to

improve the finishing of printed parts in PLA, (Marnix, 2014).

To improve surface quality and to ensure airtightness of printed parts in NinjaFlex®, a mixture of a flexible polyurethane-based adhesive called *Loctite Vinyl, Fabric & Plastic Flexible Adhesive*, with a solvent called MEK-methyl ethyl ketone is used. MEK is a universal solvent. At least 25% of MEK, by volume, to sufficiently reduce the viscosity of the mixture and optimize the deposition of the airproofing film.

Stereoscopic Microscopy:

A stereomicroscopic microscope, Nikon SMZ645, and a microscope camera, Moticam 10, were used to characterize the surface morphology of the printed samples without any processing and after covering with airproofing film. The images acquired with the camera will allow to infer about the effectiveness of the airproofing film.

The NinjaFlex® sample obtained by 3D printing was characterized by stereoscopic microscopy. Figure 3.1 shows the surface morphology constituted by parallelly aligned cylindrical filaments, with a thickness less than 100 µm. Faults in the alignment of the polymer filaments are visible, which are responsible for the lack of airtightness.

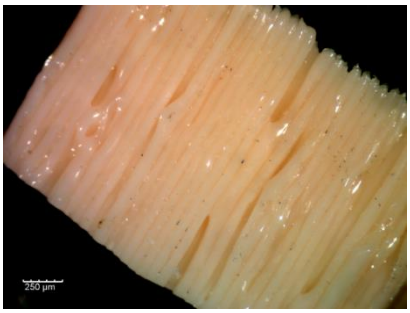

Figure 3.1 - Sample without airproofing film - stereoscopic microscopy

Figure 3.2 shows the sample image after covering with the airproofing film (Loctite Vinyl, Fabric & Plastic Flexible Adhesive + MEK). The reduction of surface roughness due to the film effect is visible. The spaces between the filaments disappear and the juxtaposition faults of the filaments are closed. The image shows small air bubbles formed during the mixing of the glue with MEK due to the high viscosity of the glue and the resulting mixture.

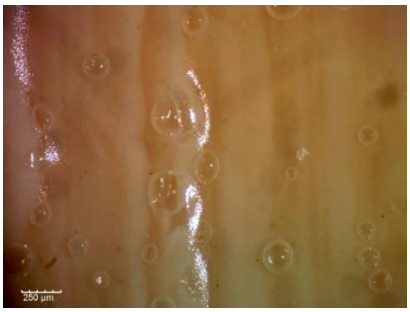

Figure 3.2 – Sample after coverage with airproofing film - stereoscopic microscopy

It was also found that the printed sample when contacted with the pure solvent (MEK) achieves a better surface smoothing, as shown in Figure 3.3. However, this smoothing is not effective in closing the stacking flaws of the filaments, thus not guaranteeing the airtightness of the sample.

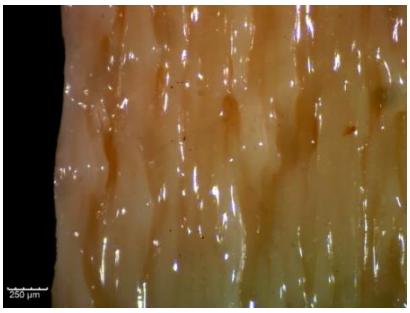

Figure 3.3 - Sample after coverage with pure MEK - stereoscopic microscopy

3.2. BASE MODEL

Considering the improvement of the proposed geometry and the limitations of the printer, the base model of the pneumatic actuator is shown in Figure 3.4.

Figure 3.4 – Base Model

Figure 3.5, shows the computational model compared with the real deformed model, both with internal pressure of 2.15 bar. At this pressure level, using the same method to calculate the bending angle as used in Section 2, the actuator bends 211.3°. As seen, if more pressure is introduced, more deformation is achieved.

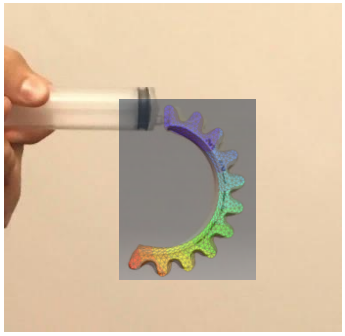

Figure 3.5 – Comparison between the real model and the ABAQUS® model

3.3. Model with Anatomical Approximation

In this model, geometry is improved to be to be similar to a finger. For this, it is intended to concentrate the deformation (bending) near the anatomical joints, leaving the distal phalanges, intermediate phalanges and proximal phalanges as non-deformable. The thickness of the wall is reduced (from 1.2mm to 0.8mm) and a reduction of the EFD's is done, i.e., the dimension of the radius is reduced, in order to have a greater number of EFD's in the same space. The actuator is shown in Figure 3.6.

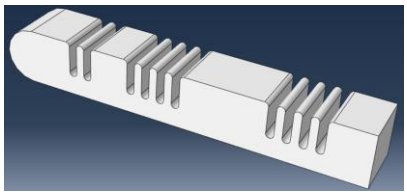

Figure 3.6 – Actuator with anatomical approximation

Defining the internal pressure equal to 2.5 bar, gives the response shown in Figure 3.7 (A). It can be concluded, using the same method to calculate the bending angle, as previously, that the actuator bends 168.1°. Figure 3.7 (A) and Figure 3.7 (B) show that the bending angle of the actuator is very similar to the maximum bend angle a human finger can perform.

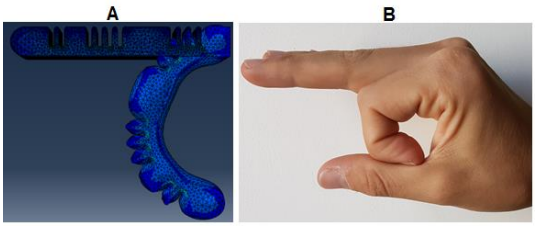

Figure 3.7 – Comparison of A: Actuator with anatomical approach response; with B: Human finger bending

4. Prototype

In this chapter a prototype of a system that allows to show the concept of the actuator is developed. This prototype must have the capacity to deal with at least 2 bar. The initial idea was to search the market for pneumatic compressors, which were at the same time lightweight, efficient and capable of generating the necessary pressure. It was found that these solutions were not available because either they were too heavy or didn't produce the necessary pressure. Taking advantage of the 3D printing capabilities, which enable rapid prototyping, and with a syringe, a leadscrew and a stepper motor, that pressure is produced.

4.1. Components Selection

To produce the prototype the components presented in the Table 4.1 were selected.

Table 4.1 – Prototype components

Component	Reference
Stepper Motor	Pololu® Unipolar/Bipolar, 200 Steps/Rev, 57×41mm, 5.7V, 1 A/Phase
Leadscrew	IGUS® DST-LS-6.35X5.08-R-ES
Nut	IGUS® DST-JFRM-1315DS6.35X5.08
Syringe	30 ml
Arduino	Arduino Uno v3
Motor controller	L298N Dual Motor Controller Module
Speed control Sensors	FSR 402 – Force Sensitive Resistor
Stop Sensors	MA-153 event switches

The other components were 3D printed with rigid materials, PLA and ABS.

4.2. System Characterization

To calculate the force that the actuator can achieve, a very rudimentary experimental apparatus was assembled, composed of the actuation system and a scale. The actuator exerts pressure on the scale and the last emits the value of the weight caused by that pressure.

With the motor running at its maximum speed, 300 RPM, the actuator bends fully in approximately 3 seconds and exerts a force of approximately 0.7 N.

A comparative analysis between the piston speed and the speed of the actuator tip, with different motor rotation speeds, was also made, see Table 4.2.

Table 4.2 - Comparison between the piston and actuator end speeds with different motor speeds

MOTOR speed [rpm]	Leadscrew / piston speed [mm/s]	Actuator tip average speed [mm/s]
100	8.47	7.31
150	12.70	10.70
200	16.93	14.20
250	21.17	17.85
300	25.40	21.23

This comparison shows that the piston speed and the actuator tip average speed vary linearly with the motor rotation speed. When the plunger movement begins, the actuator begins to be inflated until at a certain point when it begins to bend. While no bending occurs, the actuator does not move, so the average speed of the actuator tip is affected.

The grip control is based on the failsafe concept, in which, in the absence of actuation, the system remains in its position, for safety proposes. This solution can be discussed from the biomechanical point of view, but this allows to alleviate the possibility of muscular fatigue of the user. Another type of concepts / control is beyond the objectives of this work and should be studied in future works.

5. CONCLUSIONS AND FUTURE WORK

5.1. CONCLUSIONS

In this work pneumatic actuators are developed, using advanced additive manufacturing techniques, which can be used for orthoses or prostheses. To understand the importance of these devices, some examples of the application of pneumatic actuators were presented together with a brief historical evolution of technical aids.

Due to the large deformations that occur in the actuators and the nonlinear properties of their materials, simple linear models do not accurately describe their mechanical behaviour. For this, more advanced modelling and simulation techniques are required. In order to understand the parameters that most influence the bending / deformation of the actuator, the actuator was computationally modelled, (geometric modelling-Solidworks® and finite element modelling-ABAQUS®). Through an iterative process, the best configuration of the actuator was achieved. This iterative process consisted in independently varying a single geometric parameter at a time. The response of each of the iterations, given by the software of finite elements, allowed to perform a sensitivity analysis to estimates the sensitivity of the results to a certain parameter. It has been shown that the parameters that most influence the bending / deformation of the actuator are: pressure, wall thickness, radius dimension and number of EFD's.

There are many 3D printed technical aids, some of which are presented in this work. From the previous study (computational modelling of pneumatic actuators), resulted the 3D printed pneumatic actuators: the base model, which is the actuator with better configuration, i.e., that presented greater deformation when subjected to an internal pressure; and the model with anatomical approximation, which is an actuator with similarities to a human finger. In this model our intend was to focus the deformation near the anatomical joints, leaving the distal phalanges, intermediate phalanges and proximal phalanges as non-deformable. From these prints, result ideal conditions for printing the actuators in NinjaFlex® that guarantee that they are airtight.
For these actuators, in the Lulzbot® TAZ 6, double-extrusion printing is not recommended, neither support material (internal or external) should be used and material retraction should not be used. From the work done came less good results, highlighting the test with water that causes unwanted changes in the material properties.

The 3D printed actuator works, but it is not durable without post-processing. In this work a novel post-processing method is presented. First tests clearly demonstrate the potential to improve the quality of the surface and airtightness.

To finalize the work, the physical prototype of the system is presented. The

components have been designed, so that the prototype works. With this prototype and the anatomical approximation model, forces of 0.7N can be obtained and the system can bend the actuator in approximately 3s (300 RPM). The grip control is based on the failsafe concept, in which, in the absence of actuation, the system remains in its position, for safety proposes.

5.2. FUTURE WORK

The area of prosthetics and orthotics with the use of additive manufacturing, has developed a lot in recent years. Lately, with the printing of flexible materials, these prostheses resemble even more the members of the human body. 3D printed flexible prosthetics, based on the pneumatic concept, are still under developed and need further improvements – making it possible to envision new prosthetics systems to help people with needs in that respect.

The developed actuators, due to being operated with air, which is highly compressible, have a very low efficiency. In future works, in the actuation system, a liquid can be used, for example oil, which is incompressible. It improves efficiency and it would require much less volume of liquid to make the actuation, and would achieve larger grip forces.

In the presented work, as mentioned, grip control is based on the concept of failsafe. In future works this prehension paradigm can be studied, in the sense of making it more similar to the one that humans present. For example, picking up an object: an individual with no pathologies can grasp the object and have the sensitivity to do only the necessary gripping force in order to hold the object; an individual who has a pathology (congenital or amputation) can't control this same gripping force.

Finally, it is possible to suggest a computational study using the finite element method of the gripping force that the actuator can do, i.e. with different pressure values, it is possible to predict the force that the actuator allows to do. This study is quite useful as it allows for example to obtain Force vs. Pressure graphs and use this data for the final product.

6. REFERENCES

Desmond, D. M. and MacLachlan, M. (2006) 'Coping strategies as predictors of psychosocial adaptation in a sample of elderly veterans with acquired lower limb amputations', *Social science & medicine*. Pergamon, 62(1), pp. 208–216.

Kim, S., Laschi, C. and Trimmer, B. (2013) 'Soft robotics: a bioinspired evolution in robotics', *Trends in Biotechnology*. Elsevier, 31(5), pp. 287–294. doi: 10.1016/j.tibtech.2013.03.002.

Laschi, C. and Cianchetti, M. (2014) 'Soft Robotics: New Perspectives for Robot Bodyware and Control', *Frontiers in bioengineering and biotechnology*. Frontiers Media S.A., 2, p. 3. doi: 10.3389/fbioe.2014.00003.

Marnix (2014) *Smoothing PLA*. Available at: http://fabsterdam.com/3dprinting/smoothing-pla/ (Accessed: 26 September 2017).

Michael Graham (2015) *Effect of Acetone Vapor Polishing on 3D Printed ABS Parts*. Available at: https://engineerdog.com/2015/05/04/effect-of-acetone-vapor-polishing-on-3d-printed-abs-parts/ (Accessed: 26 September 2017).

O'Neill, C. T., Phipps, N. S., Cappello, L., Paganoni, S. and Walsh, C. J. (2017) 'A soft wearable robot for the shoulder: Design, characterization, and preliminary testing', in *Rehabilitation Robotics (ICORR), 2017 International Conference on*. IEEE, pp. 1672–1678.

Payne, C. J. *et al.* (2017) 'Wearable Soft Robotic Device Supports the Failing Heart In Vivo', in *The 9th Hamlyn Symposium on Medical Robotics*. London, June 25-28.

Wilson, J. F. (1988) 'Fluid actuated limb'. Google Patents. Available at: https://www.google.com/patents/US4792173.

Yap, H. K., Ng, H. Y. and Yeow, C. H. (2016) 'High-Force Soft Printable Pneumatics for Soft Robotic Applications', *Soft Robotics*. Mary Ann Liebert, Inc. 140 Huguenot Street, 3rd Floor New Rochelle, NY 10801 USA, 3(3), pp. 144–158.